

## Emergence of Chaos in Quantum Systems Far from the Classical Limit

Salman Habib,<sup>1</sup> Kurt Jacobs,<sup>1,2</sup> and Kosuke Shizume<sup>3</sup>

<sup>1</sup>*MS B285, Theoretical Division, The University of California, Los Alamos National Laboratory, Los Alamos, New Mexico 87545, USA*

<sup>2</sup>*Centre for Quantum Computer Technology, Centre for Quantum Dynamics, School of Science, Griffith University, Nathan 4111, Australia*

<sup>3</sup>*Institute of Library and Information Science, University of Tsukuba, 1-2 Kasuga, Tsukuba, Ibaraki 305-8550, Japan*

(Received 11 April 2005; published 10 January 2006)

The dynamical status of isolated quantum systems is unclear as conventional measures fail to detect chaos in such systems. However, when quantum systems are subjected to observation—as all experimental systems must be—their dynamics is no longer linear and, in the appropriate limit(s), the evolution of expectation values, conditioned on the observations, closely approaches the behavior of classical trajectories. Here we show, by analyzing a specific example, that microscopic continuously observed quantum systems, even far from any classical limit, can have a positive Lyapunov exponent, and thus be truly chaotic.

DOI: 10.1103/PhysRevLett.96.010403

PACS numbers: 05.45.Mt, 03.65.Ta, 05.45.Pq

There can be no chaos in the dynamics of bounded and isolated (or closed) quantum systems. This is because quantum evolution is necessarily quasiperiodic, a direct consequence of the discrete spectrum of the quantum Liouville equation [1]. This leads to a widely recognized difficulty, as classical mechanics, which manifestly exhibits chaos, must emerge from quantum mechanics in an appropriate macroscopic limit [2]. The key to the resolution of this apparent paradox lies in the fact that all experimentally accessible situations necessarily involve measured, open systems: the central importance of such situations in the context of chaos was first emphasized by Chirikov [3]. In a parallel development, continuous quantum measurement theory [4] has led to the successful understanding of the emergence of classical dynamics from the underlying quantum physics [5–8], and inequalities have been derived that encapsulate the regime under which classical motion, and thus classical chaos, exist [6]. The transition to classical mechanics results from the localization of the density matrix due to the information continuously provided by the measurement (itself mediated by an environmental interaction), and the balancing of this against the unavoidable noise from the quantum backaction of the measurement. For a macroscopic system, the Ehrenfest theorem holds as a result of localization and, simultaneously, the backaction noise is negligible, resulting in a smooth classical trajectory.

While it has been established that observed quantum systems can be chaotic when they are macroscopic enough that classical dynamics has emerged, can they be chaotic outside this limit? This is the question we address here. By defining and computing the Lyapunov exponent for an observed quantum system deep in the quantum regime, we are able to show that the system dynamics is chaotic. Further, the Lyapunov exponent is not the same as that of the classical dynamics that emerges in the classical limit. Since the quantum system in the absence of measurement is not chaotic, this chaos must emerge as the strength of the

measurement is increased, and we examine the nature of this emergence.

Chaos is quantified in a dynamical system by the maximal Lyapunov exponent [9]. The exponent yields the (asymptotic) rate of exponential divergence of two trajectories which start from neighboring points in phase space, in the  $t \rightarrow \infty$  limit, the points staying infinitesimally close. The maximal Lyapunov exponent characterizes the sensitivity of the evolution to changes in the initial condition: if it is positive, then the system is exponentially sensitive to initial conditions, and is said to be chaotic. We apply this notion below to the observation-conditioned evolution of quantum expectation values.

The evolution of a simple single-particle quantum system under an ideal continuous position measurement is given by the nonlinear stochastic master equation (SME) for the system density matrix [10]:

$$d\rho = -\frac{i}{\hbar}[H, \rho]dt - k[x, [x, \rho]]dt + 4k(x\rho + \rho x - 2\langle x \rangle)(dy - \langle x \rangle dt), \quad (1)$$

where the first term on the right-hand side is due to unitary evolution,  $H$  being the Hamiltonian, and the second term represents diffusion from “quantum noise” due to the unavoidable quantum backaction of the measurement. The position operator is  $x$ , and the parameter  $k$  characterizes the rate at which the measurement extracts information about the observable, and which we will refer to as the *strength* of the measurement [11]. The final term represents the change in the density matrix as a result of the information gained from the measurement. Here,  $dy$  is the infinitesimal change in the continuous output of the measuring device in the time  $dt$ . The continuous output of the measuring device,  $y(t)$ , referred to usually as the *measurement record*, is determined by  $dy = \langle x \rangle dt + dW/\sqrt{8k}$ , where  $dW$  is the Wiener increment, describing driving by Gaussian white noise [12]. The noise  $dW$  is due to the fact

that the results of the measurement are necessarily random. (Note that the backaction and  $dW$  are uncorrelated with each other.) Thus on a given experimental run, the system will be driven by a given realization of the noise process  $dW$ . We will label the possible noise realizations by  $s$ . The SME (1) is valid for measurements on a wide range of systems, and imposes no restrictions on the strength of the measurement backaction, so long as the probe and system time scales are widely separated and damping due to the probe can be neglected.

A single quantum mechanical particle is in principle an infinite dimensional system. However, for the purpose of defining an observationally relevant Lyapunov exponent, it is sufficient to use a single projected data stream: Here we choose the expectation value of the position,  $\langle x(t) \rangle$ . The important quantity is thus the divergence,  $\Delta(t) = |\langle x(t) \rangle - \langle x_{\text{fid}}(t) \rangle|$ , between a fiducial trajectory and a second “shadow” trajectory infinitesimally close to it. It is important to keep in mind that the system is driven by noise. Since we wish to examine the sensitivity of the system to changes in the initial conditions, and not to changes in the noise, we must hold the noise realization fixed when calculating the divergence. The Lyapunov exponent is thus

$$\lambda \equiv \lim_{t \rightarrow \infty} \lim_{\Delta_s(0) \rightarrow 0} t^{-1} \ln \Delta_s(t) \equiv \lim_{t \rightarrow \infty} \lambda_s(t), \quad (2)$$

where the subscript  $s$  denotes the noise realization. This definition is the obvious generalization of the conventional ordinary differential equation definition to dynamical averages, where the noise is treated as a drive on the system. Indeed, under the conditions when (noisy) classical motion emerges, and thus when localization holds (Fig. 1), it reduces to the conventional definition, and yields the correct classical Lyapunov exponent. To combat slow convergence, we measure the Lyapunov exponent by averaging over an ensemble of finite-time exponents  $\lambda_s(t)$  instead of taking the asymptotic long-time limit for a single trajectory.

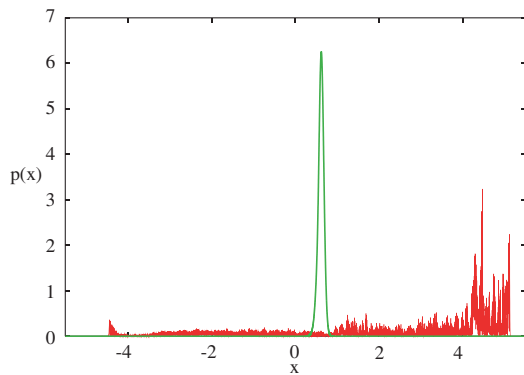


FIG. 1 (color). Position distribution for the Duffing oscillator with measurement strengths  $k = 0.01$  (red) and  $k = 10$  (green), demonstrating measurement-induced localization ( $k = 10$ ). The momentum distribution behaves similarly.

It is important to note that this definition of the Lyapunov exponent is not merely a formal result; the exponent can be obtained experimentally from measurements on a real system as in next-generation cavity QED and nanomechanics experiments [13]. The procedure is as follows. Experimentally, one would use the known measurement record to obtain the fiducial trajectory. Knowing the system Hamiltonian, one then calculates the Lyapunov exponent by following a shadow trajectory using the same  $dW$  as that of the measured fiducial trajectory.

A key result follows from our definition of the exponent. For unobserved, i.e., isolated quantum systems, it is possible to prove, by employing unitarity and the Schwarz inequality that, as expected,  $\lambda$  vanishes and further that the finite-time exponent,  $\lambda(t)$ , decays away as  $1/t$  [14]. As we have emphasized earlier, however, once measurement is included the evolution becomes nonlinear and the Lyapunov exponent need not vanish. We now address this crucial question for a specific example.

The system we consider is the quantum Duffing oscillator [15], which is a single particle in a double-well potential, with sinusoidal driving. The Hamiltonian for the Duffing oscillator is

$$H = p^2/2m + Bx^4 - Ax^2 + \Lambda x \cos(\omega t), \quad (3)$$

where  $p$  is the momentum operator;  $m$  the particle mass; and  $A$ ,  $B$ , and  $\Lambda$  determine the potential and the strength of the driving force. We fix the values of the parameters to be  $m = 1$ ,  $B = 0.5$ ,  $A = 10$ ,  $\Lambda = 10$ , and  $\omega = 6.07$ . The action of a system relative to  $\hbar$  can be varied either by changing parameters in the Hamiltonian, or by introducing scaled variables so that the Hamiltonian remains fixed, but the effective value of  $\hbar$  becomes a tunable parameter. Here we employ the latter choice as it captures the notion of system size with a single number; the smaller  $\hbar$  the larger the system size, and vice versa.

To examine the emergence of chaos we will first choose  $\hbar = 10^{-2}$ , which is small enough so that the system makes a transition to classical dynamics when the measurement is sufficiently strong. In this way, as we increase the measurement strength, we can examine the transformation from essentially isolated quantum evolution all the way to the (known) chaos of the classical Duffing oscillator. To examine the emergence of chaos, we simulate the evolution of the system for  $k = 5 \times 10^{-4}$ ,  $10^{-3}$ ,  $0.01$ ,  $0.1$ ,  $1$ ,  $10$ . When  $k \leq 0.01$ , the distribution is spread over the entire accessible region, and Ehrenfest’s theorem is not satisfied. Conversely, for  $k = 10$ , the distribution is well localized (Fig. 1), and Ehrenfest’s theorem holds throughout the evolution [16]. Since the backaction noise, characterized by the momentum diffusion coefficient,  $D_p = \hbar^2 k$ , remains small, at this value of  $k$  the motion is that of the classical system, to a very good approximation.

Stroboscopic maps help reveal the global structural transformation in phase space in going from quantum to classical dynamics (Fig. 2). The maps consist of points

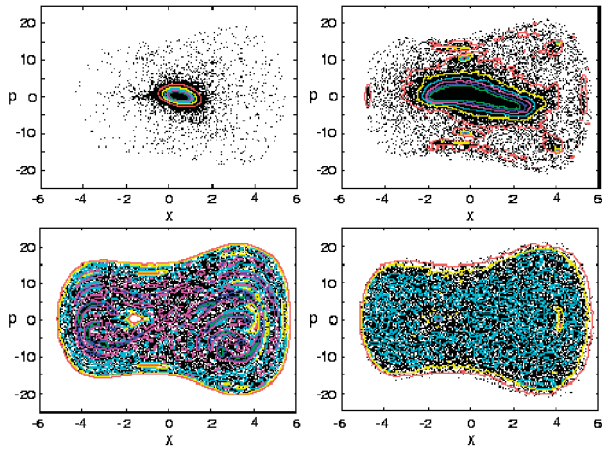


FIG. 2 (color). Phase-space stroboscopic maps shown for 4 different measurement strengths,  $k = 5 \times 10^{-4}$ , 0.01 (top), and 1, 10 (bottom). Contour lines are superimposed to provide a measure of local point density at relative density levels of 0.05, 0.15, 0.25, 0.35, 0.45, and 0.55.

through which the system passes at time intervals separated by the period of the driving force. For very small  $k$ ,  $\langle x \rangle$  and  $\langle p \rangle$  are largely confined to a region in the center of phase space. Somewhat remarkably, at  $k = 0.01$ , although the system is largely delocalized as shown in Fig. 1, nontrivial structure appears, with considerable time being spent in certain outer regions. By  $k = 1$  the localized regions have formed into narrower and sharper swirling coherent structures. At  $k = 10$  the swirls disappear, and we retrieve the uniform chaotic sea of the classical map (the small “holes” are periodic islands). The swirls in fact correspond to the unstable manifolds of the classical motion. Classically, these manifolds are only visible at short times, as continual and repeated folding eventually washes out any structure in the midst of a uniform tangle. In the quantum regime, however, the weakness of the measurement, with its inability to crystallize the fine structure, has allowed them to survive: we emphasize that the maps result from long-time integration, and are therefore essentially time invariant.

To calculate the Lyapunov exponent we implement a numerical version of the classical linearization technique [17], generalized to quantum trajectories. The method was tested on a classical noisy system against results from solving the exact equations for the exponents [18]. The calculation is very numerically intensive, as it involves integrating the stochastic Schrödinger equation equivalent to the SME (1) over thousands of driving periods, and averaging over many noise realizations; parallel supercomputers were invaluable for this task.

We find that as  $t$  is increased, for nonzero  $k$ , the value obtained for  $\lambda(t)$  falls as  $1/t$ , following the behavior expected for  $k = 0$ , until a point at which an asymptotic regime takes over, stabilizing at a finite value of the Lyapunov exponent as  $t \rightarrow \infty$ . This behavior is shown in Fig. 3 for three different values of  $k$ . The Lyapunov exponent as a function of  $k$  is shown in Fig. 4. The exponent

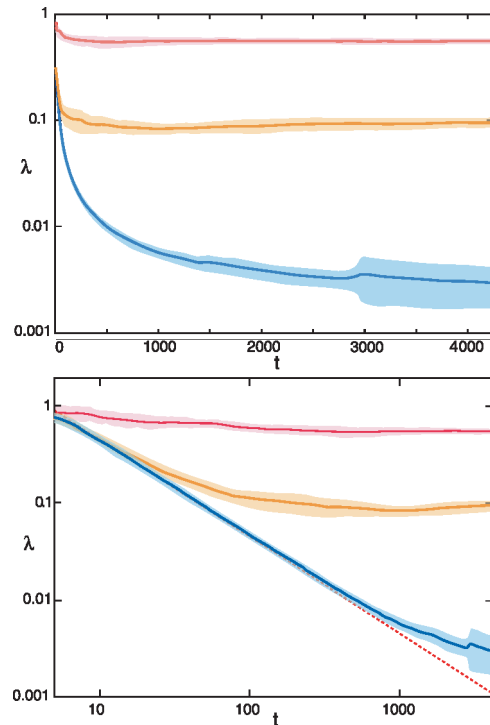


FIG. 3 (color). Finite-time Lyapunov exponents  $\lambda(t)$  for measurement strengths  $k = 5 \times 10^{-4}$ , 0.01, 10, averaged over 32 trajectories for each value of  $k$  (linear scale in time, top, and logarithmic scale, bottom; bands indicate the standard deviation over the 32 trajectories). The (analytic)  $1/t$  falloff at small  $k$  values, prior to the asymptotic regime, is evident in the bottom panel. The unit of time is the driving period.

increases over 2 orders of magnitude in an approximately power-law fashion as  $k$  is varied from  $5 \times 10^{-4}$  to 10, before settling to the classical value,  $\lambda_{\text{Cl}} = 0.57$ . The results in Figs. 3 and 4 show clearly that chaos emerges in the observed quantum dynamics well before the limit of classical motion is obtained.

We now compute the Lyapunov exponent for the quantum system when its action is sufficiently small that smooth classical dynamics cannot emerge, even for strong measurement. Taking a value of  $\hbar = 16$ , we find that for  $k = 5 \times 10^{-3}$ ,  $\lambda = 0.029 \pm 0.008$ , for  $k = 0.01$ ,  $\lambda = 0.048 \pm 0.016$  and for  $k = 0.02$ ,  $\lambda = 0.089 \pm 0.02$ . Thus the system is once again chaotic, and becomes more strongly chaotic the more strongly it is observed. From these results, it is clear that there exists a purely *quantum* regime in which an observed system, while behaving in a fashion quite distinct from its classical limit, nevertheless evolves chaotically with a finite Lyapunov exponent, also distinct from the classical value.

It is worth pointing out that an analogous analysis can be carried out for a continuously observed classical system. First we define an *unobserved* classical system as one where the observer has access to a phase space probability density for the system, but no access to individual particle trajectories. In this case, trajectories only arise if an observer makes measurements on the system in close analogy

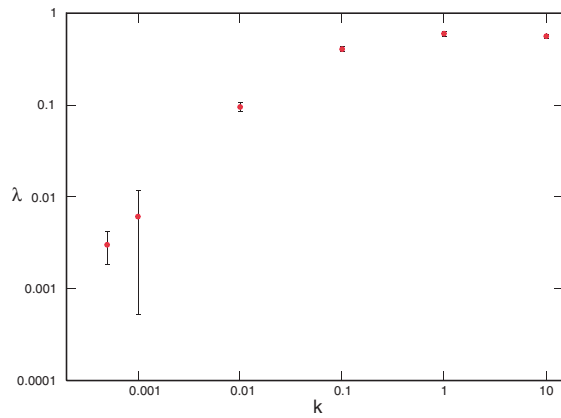


FIG. 4 (color). The emergence of chaos: The Lyapunov exponent  $\lambda$  as a function of measurement strength  $k$ . Error bars follow those of Fig. 3, taken at the final time.

to the quantum situation studied above. It can be shown that in the unobserved case the average of  $x$  for an ensemble of particles does not exhibit chaos [14].

In a classical system the external noise is not connected to the strength of the measurement, so one can simultaneously have strong measurement and weak noise, which is possible in the quantum theory only under specific conditions [6]. If we consider a noiseless observed chaotic classical system, then even a weak measurement will, over time, localize the probability density, generating an effective trajectory limit for  $\langle x(t) \rangle$  possessing the classical Lyapunov exponent,  $\lambda_{\text{Cl}}$  [14].

When the noise is sufficiently weak,  $\lambda_{\text{Cl}}$  will once again be recovered by a continuous measurement. As one way to understand this case, we can employ the quantum result as an intermediate step. Consider the quantum Lyapunov exponent at a fixed value of  $k$  (where  $\lambda < \lambda_{\text{Cl}}$ ) as in Fig. 4. If the value of  $\hbar$  is now reduced, the observed dynamics must tend to the classical limit as the quantum-classical correspondence inequalities of Ref. [6] are better satisfied. Thus the Lyapunov exponent in the classical limit of quantum theory—which, to a very good approximation, is just classical dynamics driven by weak noise—must tend to  $\lambda_{\text{Cl}}$ . If, however, the noise is not weak, observed classical dynamics, like that of a quantum system outside the classical regime, will also not be localized, and  $\langle x(t) \rangle$  may well have an exponent different from  $\lambda_{\text{Cl}}$ . In addition, one may expect the nonlocalized quantum and classical evolutions to have quite different Lyapunov exponents for  $\langle x(t) \rangle$ , especially when  $\hbar$  is large on the scale of the phase space, as quantum and classical evolutions generated by a given nonlinear Hamiltonian are essentially different [19]. The nature of the Lyapunov exponent for nonlocalized classical systems, and its relationship to the exponent for quantum systems is a very interesting open question.

We thank Tanmoy Bhattacharya, Daniel Steck, and James Theiler for helpful suggestions. Supercomputing resources were made available by the LANL Institutional

Computing Initiative and the Queensland Parallel Supercomputing Facility. This work was supported by the DOE, the ARC, JSPS, and the state of Queensland.

- 
- [1] R. Kosloff and S. A. Rice, *J. Chem. Phys.* **74**, 1340 (1981); J. Manz, *J. Chem. Phys.* **91**, 2190 (1989).
  - [2] See, e.g., A. Peres, *Quantum Theory: Concepts and Methods* (Kluwer, London, 1993).
  - [3] B. V. Chirikov, *Chaos* **1**, 95 (1991).
  - [4] H. J. Carmichael, *An Open Systems Approach to Quantum Optics* (Springer, Berlin, 1993); C. W. Gardiner and P. Zoller, *Quantum Noise* (Springer, Berlin, 2000); M. Orszag, *Quantum Optics* (Springer, Berlin, 2000).
  - [5] T. P. Spiller and J. F. Ralph, *Phys. Lett. A* **194**, 235 (1994); T. A. Brun, I. C. Percival, and R. Schack, *J. Phys. A* **29**, 2077 (1996); W. T. Strunz and I. C. Percival, *J. Phys. A* **31**, 1801 (1998).
  - [6] T. Bhattacharya, S. Habib, and K. Jacobs, *Phys. Rev. Lett.* **85**, 4852 (2000); *Phys. Rev. A* **67**, 042103 (2003); See also, S. Ghose *et al.*, *Phys. Rev. A* **69**, 052116 (2004).
  - [7] A. J. Scott and G. J. Milburn, *Phys. Rev. A* **63**, 042101 (2001).
  - [8] Y. Ota and I. Ohba, *Phys. Rev. E* **71**, 015201 (2005).
  - [9] J.-P. Eckmann and D. Ruelle, *Rev. Mod. Phys.* **57**, 617 (1985).
  - [10] L. Diosi, *Phys. Lett. A* **129**, 419 (1988); V. P. Belavkin and P. Staszewski, *Phys. Lett. A* **140**, 359 (1989); Y. Salama and N. Gisin, *Phys. Lett. A* **181**, 269 (1993); H. M. Wiseman and G. J. Milburn, *Phys. Rev. A* **47**, 642 (1993); G. J. Milburn, *Quantum Semiclass. Opt.* **8**, 269 (1996); A. C. Doherty and K. Jacobs, *Phys. Rev. A* **60**, 2700 (1999).
  - [11] A. C. Doherty, K. Jacobs, and G. Jungman, *Phys. Rev. A* **63**, 062306 (2001).
  - [12] This idealized measurement has an output record with infinite bandwidth. It is a good approximation to real measurements so long as the bandwidth of the measuring device is large compared to that of the system dynamics.
  - [13] H. Mabuchi and A. C. Doherty, *Science* **298**, 1372 (2002); M. D. LaHaye, O. Buu, B. Camarota, and K. C. Schwab, *Science* **304**, 74 (2004).
  - [14] S. Habib, K. Jacobs, and K. Shizume (to be published).
  - [15] W. A. Lin and L. E. Ballentine, *Phys. Rev. Lett.* **65**, 2927 (1990); S. Habib, K. Shizume, and W. H. Zurek, *Phys. Rev. Lett.* **80**, 4361 (1998).
  - [16] See EPAPS Document No. E-PRLTAO-95-110552 for information on the numerical methodology relating to the solution of the stochastic master or Schrödinger equations and the computation of Lyapunov exponents. This document can be reached via a direct link in the online article's HTML reference section or via the EPAPS homepage (<http://www.aip.org/pubservs/epaps.html>).
  - [17] A. Wolf, J. B. Swift, H. L. Swinney, and J. A. Vastano, *Physica D (Amsterdam)* **16**, 285 (1985).
  - [18] S. Habib and R. D. Ryne, *Phys. Rev. Lett.* **74**, 70 (1995).
  - [19] S. Habib, K. Jacobs, H. Mabuchi, R. Ryne, K. Shizume, and B. Sundaram, *Phys. Rev. Lett.* **88**, 040402 (2002).